ICAST2014#Put paper number here

Adaptive bearing housing for damping treatment

Michał Lubieniecki[1], Tadeusz Uhl[1]

[1] Department of Robotics and Mechatronics, AGH-UST University of Science and Technology, Cracow, Poland

Abstract

The paper investigates the adaptive bearing housing with vibration damping capabilities. The damping in a bearing node is achieved by shunting the piezoelectric stack actuator. However, the passive shunt damping circuits are unfavorably influenced by the size and mass of the coil inductors and do not allow any adaptivity unless the coil inductor is replaced by its synthetic counterpart. The common approach to the synthetic inductance is through the operational amplifiers what still suppress the adaptivity capabilities. Instead, having the inductor in a form of switching circuit with the adaptive controller gives the possibility to adapt to the changing vibration frequencies what is especially important in case of rotating machinery. According to current researches the abovementioned shunting circuit can be implemented in a low power FPGA (field programmable gate array). Having implemented the controller structure inside a low power chip allows to exploit another specific feature of the rotating machinery i.e. work lost irrevocably in a bearing. The heat expelled in a bearing might be converted via thermoelectric phenomenon and then used to power the synthetic inductance circuitry with controller making a design fully autonomous. The proper system assumptions, and numerical investigations have been made to show the concept of autonomous vibration damper. The concept of a damper has been verified experimentally showing the system behavior in steady state conditions, while changing the rotational speed as well as during the motor startup and rundown.

1. INTRODUCTION

There has not been any attempts to combine the semi-passive piezoelectric shunted circuits (i.e. ones with synthetic inductance) with thermal harvesting sources working on internal bearing losses in rotating machines. However, some researchers have noticed the opportunity to damp out the vibration close to the bearing housing cutting the transfer path of vibrations (B. Stallaert, S. Devos, G. Pinte, W. Symens 2008). The same authors (Pinte et al. 2010) proposed the structure of the bearing node containing the flexural hinges, preload springs and stack actuators. The focus of the mentioned work was put on the damping effect with both active and passive measures. Adaptive behavior of the resultant structure was achieved with the active control system attached to it. Although also the passive vibration damping systems might

be turned autonomous what is analyzed in the following paragraphs. Assuming the vibrations are damped out via a shunted piezoelectric patch, the synthetic inductor is the only element of such system that requires external power to operate. The synthetic inductor is a circuit that has nearly constant power consumption and it has to be powered continuously to serve its function. Several types of synthetic inductors have been developed so far. First constructions were based on operational amplifiers and underwent substantial change in performance throughout the years, mainly due to advancement in electronics and scale of integration. Some authors proposed a self adaptive inductor design (Greaves et al. 2008) based on the operational amplifiers to be used in shunted piezoelectric applications. The important discovery was that despite the change in inductance the values of power consumption remained practically unchanged at the level of 100mW. It is worth to note that in this work the consumption has been obtained experimentally with no prior power optimization. A similar structure of the synthetic inductors has been tested showing power consumption at the level of 150-400 mW depending on DC bus voltage (Luo et al. 2007). The same authors proposed the synthetic inductor construction based on the power electronics instead of operational amplifiers. The result was a decrease in the power consumption by an order of magnitude. Experimental tests showed the power consumption at the level of 11mW for the value of 1H, 100kHz switching frequency and 5V DC bus.

The paper presents the analysis of the bearing housing construction able to work autonomously as an effective vibration damper. The investigated source of power supply is a thermoelectric generator eliminating the need for an external power supply. The first section of the paper describes the construction of the bearing housing that assures a high value of electromechanical coupling coefficient. Afterwards the experimentally obtained coefficient is used to calculate the damping capabilities of the investigated system. In the next paragraph the energy availability is analyzed for both the steady state and engine run-up.

2. EXPERIMENTAL SETUP

The construction of an adaptive bearing housing (Figure 1) consists of a stiff frame (1), milled pockets (2) hosting piezo actuators and disc springs, flexure hinges decoupling motion (3), mounting lugs (4) and bearing seat (5). The thermoelectric generator being an energy source of adaptive system has been mounted on the lid closing the bearing mount (not shown on the picture for clarity). There are two piezoelectric stack actuators at each direction opposed by the disc springs which preloads the actuators with adjustable force.

The preload is an important factor influencing piezo actuator effectiveness that is in turn expressed by the fraction of mode elastic strain energy stored in the piezo material. The tradeoff between bearing mount stiffness and added damping has to be found. Up to the stiffness of the stack actuator the higher preload is used the higher damping is achieved.

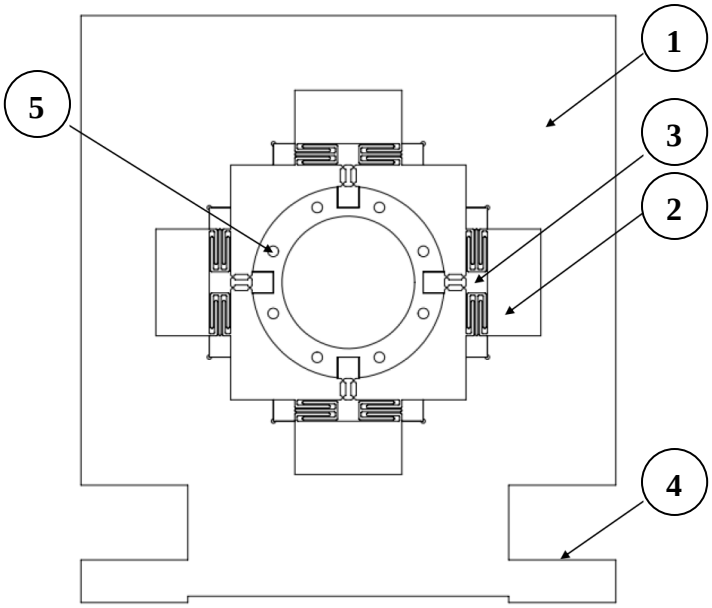

Figure 1 The view of the main construction elements of adaptive bearing housing.

The use of piezoelectric actuators requires decoupling of compressive and shear forces. A common approach is to use the flexure hinges that ensures the proper range of movement for piezoelectric stack actuators. The three types hinges have been considered (Figure 2): circular hinges for decoupling the shear forces and maze leaf springs or beam hinges for actuation. As the piezo elements cannot impose contraction forces directly, each piezo has been compressed with set of adjustable disc springs.

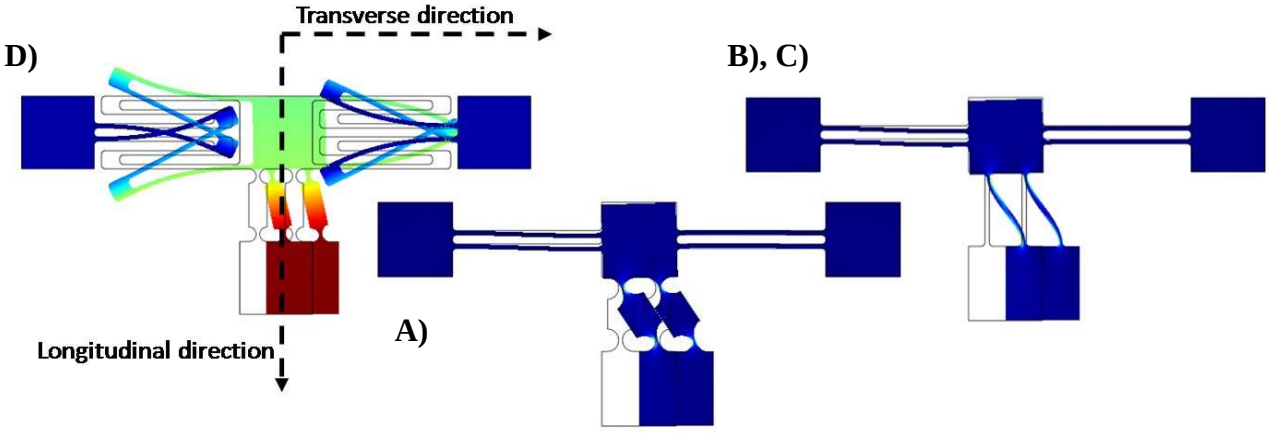

Figure 2 The shapes of the flexural hinges under investigation. The hinges variant constructions are marked as: D,A,B; C equals B with reinforced beams in longitudinal direction.

The flexure hinges were designed according to (Schotborgh et al. 2005) so that have minimal transverse stiffness, appropriately high longitudinal stiffness and assure the parallel position of mounting surfaces of

the piezo actuators under load conditions. The design assumptions and resultant coefficients for the beam hinge and circular hinge can be summarized in Table 1.

Table 1 Common assumptions and values of the design coefficient of the flexural hinges

Common assumptions	
σ_{ψ}=510E6 GPa=k_{gj}	Tensile strength, dynamic load
E=210E9 MPa	Material modulus of elasticity (50HS spring steel)
$\psi=0.5^0$ (0.0087 rad)	Angular range of hinge deflection used for calculations; The actual range of motion 50E-6 m for the hinge length L=0.02 m gives the expected deflection angle of 0.15^0 (0.0025 rad);
Beam hinge (aligned with longitudinal hinge direction)	
$\frac{\sigma_{\psi\psi}}{\psi E}=0.33$	Dimensionless number of rotation stress
$\sqrt{\frac{h}{L}}max=0.74$	The permissible shape coefficient.
$\sqrt{\frac{h}{L}}=0.1732$	The actual value of shape coeff. for the chosen design.
Beam hinge (aligned with transverse hinge direction)	
$\sqrt{\frac{h}{L}}=0.2449$	The actual value for shape coeff. for the chosen design.
Circular hinge	
$\frac{\sigma_{\psi\psi}}{\psi E}=0.28$	Dimensionless number of rotation stress
$\sqrt{\frac{h}{D}}max=0.48$	The permissible shape coefficient (max.) and the actual value for the chosen design.
$\sqrt{\frac{h}{D}}=0.25$ $\binom{h=0.0004,}{D=0.006}$	The actual value of the shape coeff. for the chosen design. To stay below the desired limit the diameter of the hinge was increased from initial 0.002 to 0.006 m.

To verify the horizontal and vertical motion decoupling the hinges design was checked in Comsol Multiphysics environment by performing following tests: static displacement-displacement analysis (based on presumed range of actuator motion), static (based on the presumed blocking force of the

actuator), buckling test, dynamic test (natural frequency analysis). The summary of the achieved flexure configuration is presented in Table 2.

Table 2 The resultant stiffness of the investigated hinges together with corresponding stress values and buckling force in performed tests. The most favorable values are marked grey.

Flexure Type*	**D**	**A**	**B**	**C**
Czz (equiv.) Beam hinge (trans.)	N/A	886e3	886e3	886e3
Czz (equiv.) Beam hinge (long.)	N/A	3.57e6	N/A	3.75e6
Cxx (equiv.) Beam hinge (long.)	N/A	9.07e8	N/A	5.00e10
Czz (equiv.) Maze hinge	N/A	N/A	N/A	N/A
Czz (equiv.) Circular hinge	6.24e6	N/A	6.24e6	N/A
Cxx(equiv.) Circular hinge	1.33e9	N/A	1.33e9	N/A
Disp-Disp [MPa]	N/A	2.060e8	3.392e8	2.170e8
Disp-Fxx [MPa]	N/A	2.652e8	4.059e8	2.790e8
F block [MPa]	N/A	0.529e8	0.540e8	0.540e8
Buckling [N]	N/A	1.17e5	4.700e5	2.71e5

*Cxx and Czz refers to the hinge coordinates (xx-longitudinal, zz-transverse). Values of Cxx and Czz stand for hinge stiffness, respectively on longitudinal and transverse direction.

Among all considered designs lowest achieved stiffness in the transverse direction and sufficient stiffness in the longitudinal direction have been achieved for flexures that base on the double beam hinge. The stack blocking force is 1800N, while free displacement is at the level of 20μm. As the expected longitudinal load that stems from the piezo blocking force may cause buckling in such hinges, therefore some reinforcement has been done. The chosen design (C) has transverse stiffness below 1N/μm, while stack stiffness is characterized by the 120N/μm. This is important as the stack has to counteract transverse stiffness of the two hinges.

3. VIBRATION DAMPING CAPABILITIES

While investigating the damping capabilities of the bearing mount two elements have to be known: the inductance in a shunted circuit and a achievable electromechanical coupling. The range of inductance has to be specified to choose which system resonant modes can be tuned to. The values of the

inductive elements corresponds to the electromechanical coupling coefficient that for simple structures might be achieved analytically in other cases the modal tests are commonly used.

The bearing dynamics can be influenced by PZT elements. During the tests the excitation was imposed by a modal hammer for both piezo terminals open and short-circuited. The tests were repeated for the excitation on shaft, housing frame and bearing seat to determine with confidence modal damping added to the system. Further investigation involved rotating shaft loaded by a screw-spring mechanism. The tests were performed for set of different loads and rotational speeds. As the housing was made symmetrical the load during tests was aligned with the axis of one chosen actuator. During these tests the possible power yield of energy harvesting system was investigated too.

The expected result of the modal testing was the shift in resonant frequencies most affected by the piezo stack. This frequency shift determine the generalized electromechanical coupling coefficient (Hagood & Von Flotow 1991) according to the formula

$$K_{ij}^2 = \frac{(\omega_n^D)^2 - (\omega_n^E)^2}{(\omega_n^E)^2} \approx \frac{k^2 v_i}{1 - k^2}$$

$$\zeta = \frac{\sqrt{K_{ij}^2}}{2}$$

where:
ω_n^D - resonant frequency (open-circuit)
ω_n^E - resonant frequency (short-circuit)
k^2 - electromechanical coupling coefficient (material dependent)
v_i - fraction of elastic strain energy stored in PZT material
K_{ij}^2 - generalized electromechanical coupling coefficient
ζ - modal damping

K_{ij}^2 shows how much of elastic strain energy is stored in piezoelectric material. The coefficient allows to quantify the maximum achievable modal damping for applied preload values. For the analyzed case the preload relations are as follows A1<A2 <A3. The presented results refers to the excitation imposed on the shaft. Although, the obtained curves (Figure 3) show different frequencies depending on the excitation location, the system inherent damping is the same in each load case. While looking onto the frequency shift (Figure 4) it is clearly visible that the piezoelectric actuator change in stiffness (while short or open circuit) cause evident change in system response. The shifted resonant peak corresponds to the bending mode of the hinges and adjoined shaft.

Table 3 Corresponding values of generalized electromechanical coupling and modal damping added to the structure together with values of inductance needed to be tuned into the addressed resonant mode.

Przypadek	K_{ij}^2	k_{31}^*	v_i	ζ	L [H]
A1	0.006799	0.7031	0.0070	0.0412	0.0347

A2	0.068120	0.7031	0.0697	0.1305	0.0155
A3	0.046584	0.7031	0.0477	0.1079	0.0147

*function of the material and actuator type (polarization)

The damping that can be applied to the resonant mode of interest is at the average level of 9% (Table 3) what can be considered a high value and can contribute significantly to lowering the amplitude of vibrations. Due to high frequency of bearing housing the needed values of the inductance are low and easily obtainable in the form of coil inductors. The bulkiness of large inductance is usually the obstacle in practical applications, here the obstacle is rather the invariability of the coil parameters that prevents any adaptive behavior.

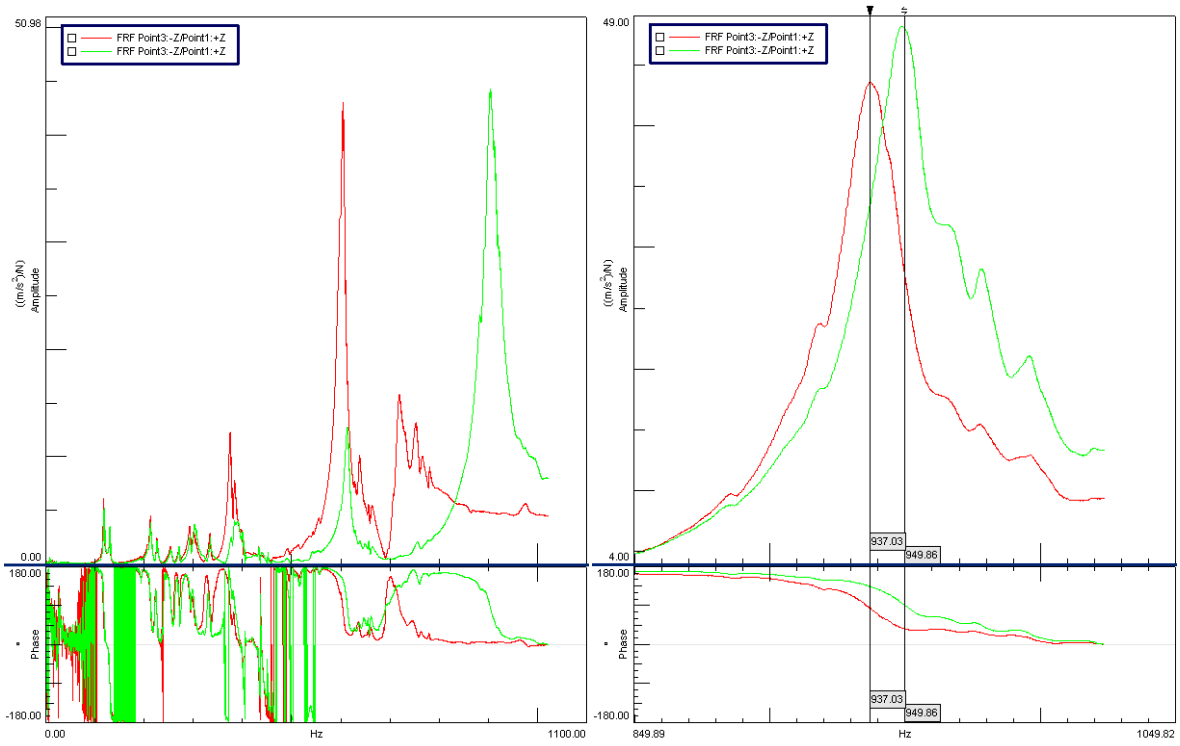

Figure 3 Left: The comparison of the response curves with the excitation imposed on the shaft (B2-red) and the bearing outer ring (A2-green); Right: The close-up view of the resonant peak for the curves obtained with different preload but the same excitation/reading point (A2-red, A3-green).

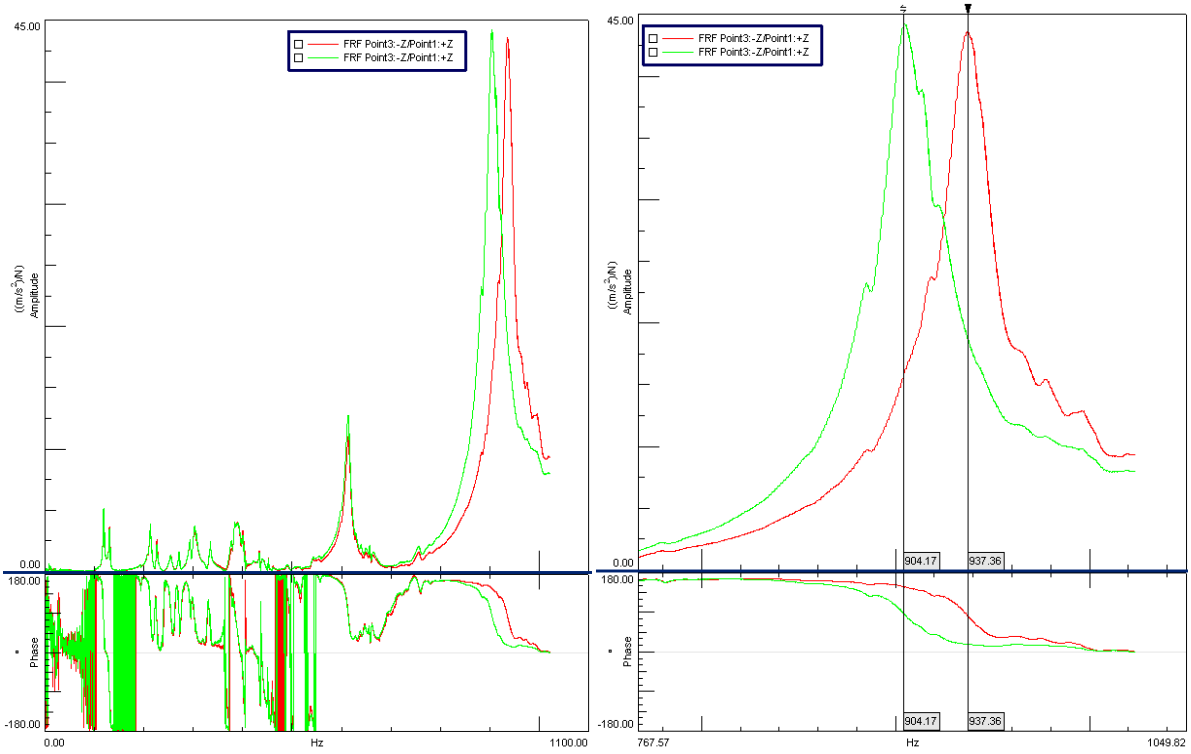

Figure 4 The comparison of the housing dynamic response for the stack actuator open- and short-circuited (A2).

4. ENERGY AVAILABILITY

In the previous research of the authors the performance prediction of the thermoelectric harvesting circuit was done based on the elaborated equivalent model of the bearing housing and adopted model of the thermoelectric source (Freunek et al. 2009). It was proven shunt circuit may be powered via the single thermoelectric generator. However, it should be noticed that this state is achieved after some time after the machine run-up. As a result the damping capabilities cannot be available at all time. For the investigated case the time after which the proper level of energy was available differs from 126-7000s for different rotational speeds and loads (Figure 5). Due to long time needed to achieve the assumed power capabilities by energy harvesting circuit some test repetitions with lowest speeds were omitted.

The tests were performed with varying speed in the range 500-3000 rpm for two load conditions: 950N and 1200N radial load. The disc spring preload didn't change throughout the test. The amount of power generated by the harvesting circuit was determined by indirect measurement of its current output (as it may be perceived as a current source). In practice the voltage on the buffer capacitor was recorded after its cyclic short-circuiting. The power threshold was set after (Luo et al. 2007) to be 11mW.

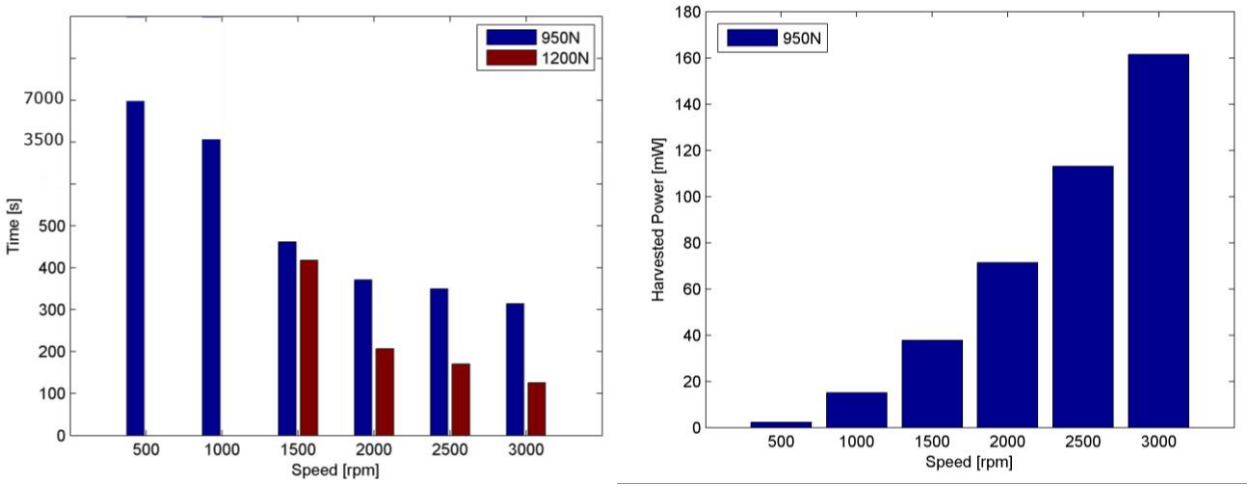

Figure 5 Left: The time needed to achieve the assumed power output by the harvesting circuit - transient response analysis; Right: The power output achieved in steady-state.

5. SUMMARY

The paper presents the consideration on energy availability of the adaptive bearing housing. It was shown that although the steady state power capacity of the harvesting circuit is sufficient to power the adaptive shunt circuit for wide range of loads and speeds, during the motor run-up the thermal capacitance prevents the system from operating for at least two minutes. Unless transition through resonance during the run-up is not crucial the adaptive bearing may be fully operational especially for the machines working continuously or intermittently with short stops. Otherwise the energy buffer is necessary. The important part of the work was to design the housing construction ensuring that the high generalized electromechanical coupling coefficient is achieved. During the tests the proper preload value has been found that allows to introduce significant modal damping to the modes of interest. The adaptive bearing housing seems to be a promising application for piezoelectric shunt damping system as it has low inherent damping.

ACKNOWLEDGMENTS

The authors acknowledge the project "The use of thermoelectric materials to improve thermal stability of high-speed rotor bearings systems", no. PBS1/A6/6/2012 financed by the National Centre for Researched and Development.

REFERENCES

B. Stallaert, S. Devos, G. Pinte, W. Symens, P.S., 2008. Active Structural Acoustic Source Control of Rotating Machinery Using Piezo Bearings. In *Proc. of 2008 IMAC-XXVI: Conference & Exposition on Structural Dynamics*.

Freunek, M. et al., 2009. New Physical Model for Thermoelectric Generators. *Journal of Electronic Materials*, 38(7), pp.1214–1220.

Greaves, M. et al., 2008. Self-optimising piezoelectric damping. *Proceedings of SPIE*, 6928, p.69282O–69282O–10.

Hagood, N.W. & Von Flotow, A., 1991. Damping of structural vibrations with piezoelectric materials and passive electrical networks. *Journal of Sound and Vibration*, 146(2), pp.243–268.

Luo, C., Whitehead, M.C. & Hofmann, H.F., 2007. Design and Testing of A Power Electronic Synthetic Inductor. *2007 IEEE Power Electronics Specialists Conference*, pp.2089–2094.

Pinte, G. et al., 2010. A piezo-based bearing for the active structural acoustic control of rotating machinery. *Journal of Sound and Vibration*, 329(9), pp.1235–1253.

Schotborgh, W.O. et al., 2005. Dimensionless design graphs for flexure elements and a comparison between three flexure elements. *Precision Engineering*, 29(1), pp.41–47.